Engineering Journal
issn: 0125-8281

Article

Creep Life Prediction for Hastelloy XR Using the Omega Method

Surat Kwanmuang[a,*] **and Jirapong Kasivitamnuay**[b]

Department of Mechanical Engineering, Faculty of Engineering, Chulalongkorn University, Thailand
E-mail: [a,*]Surat.K@chula.ac.th (Corresponding author), [b]jirapong.K@chula.ac.th

Abstract. This paper applies the Omega method to creep life prediction for Hastelloy XR at temperatures ranging from 850 to 950^{o}C in an air environment. The creep data were obtained from literature. Three life prediction scenarios were studied including constant stress, constant load, and continuous monitoring where creep data is simulated for sequential acquisition. The constant stress creep data at each temperature were used to determine the Omega model parameters, and empirical equations for each parameter were developed. The predicted creep lives under constant stress were within a factor of 2 in almost all cases. For a life prediction under constant load, the actual applied stress was estimated and used in the creep constitutive equation as well as for calculating the model parameters. The predicted creep lives were also to be within a factor of 2 in almost all cases. The Omega model was found to be applicable to a continuous creep data acquisition scenario as well. An appropriate scheme for continuous monitoring scenario was suggested, and statistical analysis by the Monte Carlo simulation was demonstrated.

Keywords: Creep, Hastelloy, Omega method.

ENGINEERING JOURNAL Volume 27 Issue 9
Received 23 March 2023
Accepted 4 September 2023
Published 30 September 2023
Online at https://engj.org/
DOI:10.4186/ej.2023.27.9.15

DOI:10.4186/ej.2023.27.9.15

1. Introduction

Creep failure is one of the life-limiting conditions for high-temperature load-bearing structural components. Since creep deformation gradually degrades components over time, estimating the remaining life of a component is required for proper management (e.g., set up inspection schedule, spare parts provision, and rerate of operational conditions). A creep life assessment of components can be divided into two broad categories [1]: 1) history-based calculation, and 2) evaluation of components in service.

In a history-based approach, the geometry and operational history of the component, as well as standard creep rupture data, are used to calculate creep damage using the damage accumulation rule (e.g., time fraction rule), and the remaining life is predicted under future operational conditions using the damage accumulation rule. This procedure tends to be inaccurate because operational conditions and material properties may not be known with sufficient accuracy. Further, there is a level of inaccuracy in the damage accumulation rule itself.

The second approach to evaluating a component in service has the potential to improve remaining life prediction because the current state of the component is examined or tested without a requirement for the past operational conditions and does not rely on standard creep properties. The evaluation can be performed using destructive or nondestructive techniques. Destructive techniques require accelerated creep or creep rupture tests of specimens prepared from the actual components. The test results are then used in conjunction with extrapolation techniques (e.g., time-temperature parameter [2], Monkman-Grant [3]) to predict the (remaining) creep life under operating conditions. Some of the disadvantages of this approach include the fact that there are always a limited number of specimens available, and data extrapolation from accelerated tests may not accurately reproduce the behavior of components [1]. Some of the techniques commonly used in practice for a nondestructive evaluation include replica metallography, hardness measurement, and strain measurement [4]. However, one advantage of strain measurement is that it can be integrated into a continuous monitoring system in situ. Numerous studies have attempted to develop a reliable measurement for strain (or deformation) using a device such as an extensometer [5], capacitive strain gauge [6], optical strain gauge [7], and electrical potential drop [8].

Since a post-service material always passes the primary and secondary creep stages, the model for a remaining creep life assessment is typically focused on creep behavior in the tertiary stage. The creep constitutive equation is used to describe or derive the creep curve, and the condition of rupture is assumed to be creep strain reaching creep ductility. Several creep constitutive equations have been proposed [9]. Kondyr et al. [10] used strain as a state variable in a tertiary creep constitutive equation. The model accurately predicted the creep life of 0.5Mo, 1Cr-0.5Mo, and 2.25Cr-1Mo steels in a temperature range of 500-600°C. Cane [11] developed a tertiary creep constitutive equation by incorporating a Kachanov-type damage evolution equation into a secondary creep behavior. Based on current strain or strain rate measurements, Cane's model could predict creep life consumption. Prager [12] redefined the meaning of parameters in the creep constitutive equation proposed by Kondyr et al. [10] and designated his approach the Omega (Ω) method. This method has been adopted in the fitness-for-service standard [13]. The Ω method has been applied successfully to a variety of steel grades and classes, including carbon steel [14], Cr-Mo steels [15-17], stainless steel [18], and superalloy [19]. However, no studies have been carried out on the applicability of this method to Hastelloy XR steel which is used in high-temperature gas-cooled reactors (HTGR) for intermediate heat exchanger heat transfer tubes and heat exchanger hot headers [20]. The service temperature of the material is estimated to be around 950°C. so a long-term creep is significant for this application.

Prager [21] reported that the parameters in the Ω model which is used for creep life prediction are relatively stable throughout life for many materials under various conditions. As a result, the Ω method can be used in a continuous remaining life assessment because the life can be predicted based on the available creep strain data up to the time of assessment. As new measurements (e.g., creep strain) are collected, the values of these parameters and remaining life are constantly updated.

This paper applied the Ω method to predict the remaining creep life of Hastelloy XR steel. First, the empirical relationships between model parameters and stresses and temperatures were established using creep data under constant uniaxial stresses at temperatures of 850, 900, and 950°C in an air environment. The relationships were then evaluated by applying them to creep data under constant stresses and constant loads. Finally, the study investigated the applicability of the Ω method in simulating the sequential gathering of creep data.

2. Background

Uniaxial creep deformation behavior can be represented graphically as a strain versus time plot, as shown in Fig. 1. Creep behavior is typically divided into three stages including primary, secondary, and tertiary, in which the creep rate decreases, remains constant, and increases with time. Time and strain at rupture are denoted as creep rupture life t_r and creep ductility ε_r, respectively.

The Ω method postulates that the tertiary stage creep rate $\dot{\varepsilon}$ is dependent on the true strain ε by the following constitutive equation.

$$\dot{\varepsilon} = \dot{\varepsilon}_0 e^{\Omega\varepsilon} \quad (1)$$

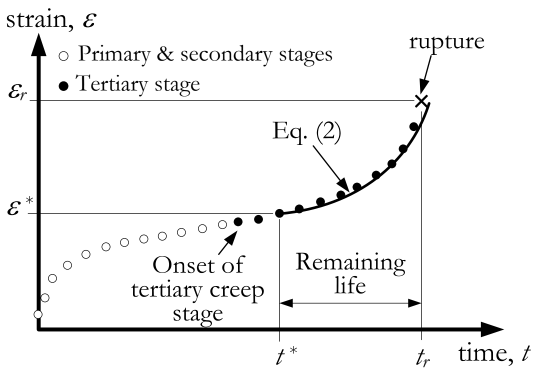

Fig. 1. Creep deformation behavior.

where Ω and the initial strain rate $\dot{\varepsilon}_0$ are parameters determined from a tertiary stage creep data.

The tertiary stage creep curve from any strain ε^* (see Fig. 1) within the tertiary creep stage can be derived from Eq. (1) as

$$\varepsilon(t) = -\frac{1}{\Omega}\ln\left[e^{-\Omega\varepsilon^*} - \dot{\varepsilon}_0\Omega(t - t^*)\right] \quad (2)$$

where t and t^* are service time and service time at strain of ε^*, respectively. At rupture, $t = t_r$ and $\varepsilon(t_r) = \varepsilon_r$ then Eq. (2) can be rearranged as

$$t_r - t^* = \frac{1}{\dot{\varepsilon}_0\Omega}\left(e^{-\Omega\varepsilon^*} - e^{-\Omega\varepsilon_r}\right), \quad (3)$$

which is the remaining life at time t^*.

Determination of the values for Ω and $\dot{\varepsilon}_0$ in Eq. (1) can be done in various ways, such as regression analysis of Eq. (2) to best fit the tertiary stage creep data, or fit the creep rate and strain in the tertiary stage as shown in Fig. (2) with the following equation:

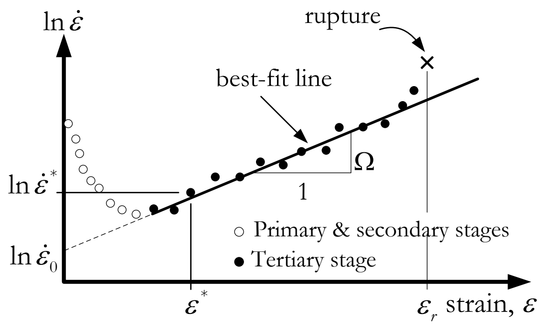

Fig. 2. Schematic of the approach to determine the parameters Ω and $\dot{\varepsilon}_0$ in the Omega model.

$$\ln\dot{\varepsilon} = \Omega\varepsilon + \ln\dot{\varepsilon}_0 \quad (4)$$

Note that Eq. (4) is a logarithmic form of Eq. (1). Parameters Ω and $\ln\dot{\varepsilon}_0$ are the slope and intercept of a best-fit line, respectively.

3. Determination of Model Parameters

Short-term creep data for Hastelloy XR used in this study was obtained from the literature [22-24]. The tests were carried out in an air environment under constant uniaxial stress and constant temperatures. Table 1 shows the test conditions and significant results including rupture time, tertiary stage onset time and strain, and creep ductility. Figures 3-5 show the creep curves at each temperature.

Table 1. Constant stress uniaxial creep data in air environment for Hastelloy XR [22-24].

Code	Temperature T (°C)	Stress σ (MPa)	Rupture time t_r (hr)	Tertiary stage: Onset time t_{ter} (hr)	Tertiary stage: Onset strain ε_{ter}	Creep ductility ε_r
CS850A-58	850	57.90	3196.80	1800.00	0.1618	0.3688
CS850A-90		89.90	199.50	110.00	0.2503	0.5372
CS850A-120		120.10	45.30	24.00	0.2759	0.6540
CS850A-170		169.80	7.60	4.67	0.4113	0.7353
CS850A-200		200.10	2.33	1.47	0.3755	0.6780
CS850A-250		250.00	0.77	0.50	0.4345	0.9623
CS900A-45	900	45.00	983.00	483.07	0.1454	0.3380
CS900A-58		58.00	267.00	143.64	0.2185	0.4090
CS900A-78		78.00	60.20	34.26	0.2454	0.5300
CS900A-100		100.00	18.60	9.99	0.3099	0.6590
CS900A-120		120.00	6.40	2.82	0.2793	0.7030
CS950A-24	950	24.01	1222.40	455.00	0.1061	0.3739
CS950A-41		41.01	164.30	94.00	0.2202	0.4166
CS950A-49		49.01	76.50	47.00	0.2620	0.4482
CS950A-62		62.02	31.03	20.00	0.3540	0.6646
CS950A-78		78.01	10.10	6.00	0.3420	0.5973
CS950A-92		92.00	5.00	2.95	0.3771	0.7147

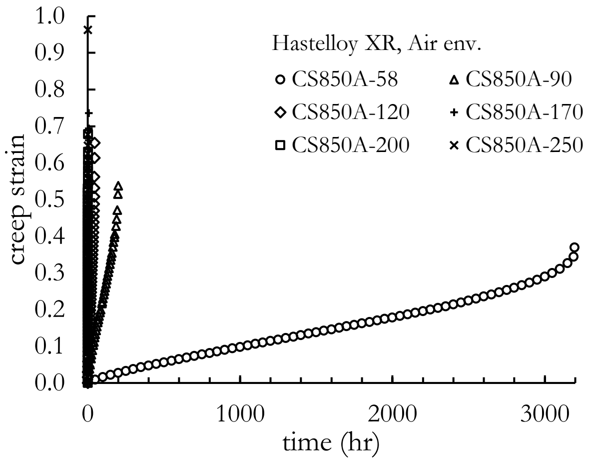

Fig. 3. Creep curves at 850°C [22].

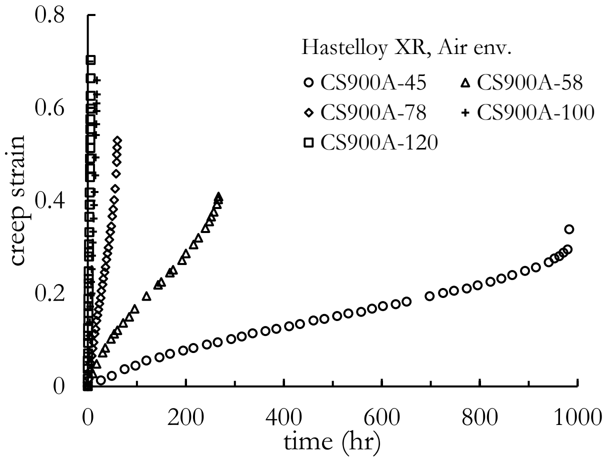

Fig. 4. Creep curves at 900°C [24].

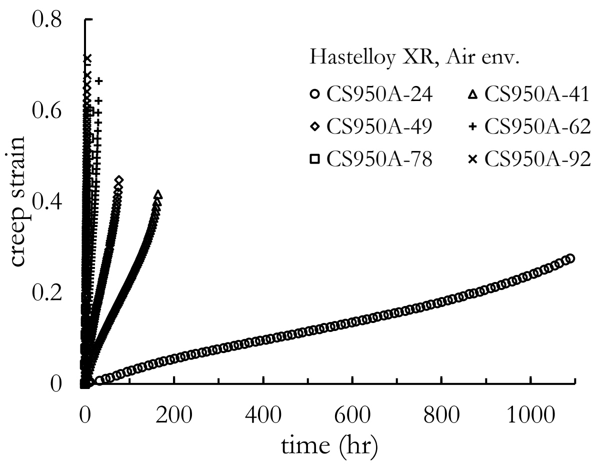

Fig. 5. Creep curves at 950°C [23].

The model parameters were determined using the method depicted in Fig. 2. Strain rate was determined by an incremental polynomial [25] instead of the central difference method used in literature to reduce scattering. The number of data points for each incremental fit of the data by a quadratic equation was set to 5 due to the limited amount of tertiary stage creep data in some cases. The creep rate for the last two data points was calculated using the central difference and backward difference methods. The natural logarithm of creep rate and corresponding creep strain at temperatures of 850, 900, and 950°C were plotted as shown in Figs. 6-8. Note that on the horizonal axis, creep strain was used instead of total strain because the instantaneous initial strain (i.e., strain at the start of loading) was negligible. These plots indicate that Eq. (4) cannot accurately fit the entire range of tertiary stage results due to the nonlinear trend. Some results, especially near the end of a test, must be discarded.

A least-square fit of a line to a group of data (i.e., $\ln(\dot{\varepsilon})$ and ε) from the onset of tertiary creep was performed with varying amounts of data ranging from three to all data in the tertiary stage. The parameters Ω and $\dot{\varepsilon}_0$ for each data group were calculated from the slope and intercept of the best-fit line and substituted into Eq. (2) to predict the tertiary stage creep curve. The creep strain prediction error was evaluated in terms of the mean absolute error (MAE), which was defined as follows:

$$MAE = \frac{1}{N_{ter}} \sum_{i=1}^{N_{ter}} \left| \varepsilon_{pred} - \varepsilon_{exp} \right| \qquad (5)$$

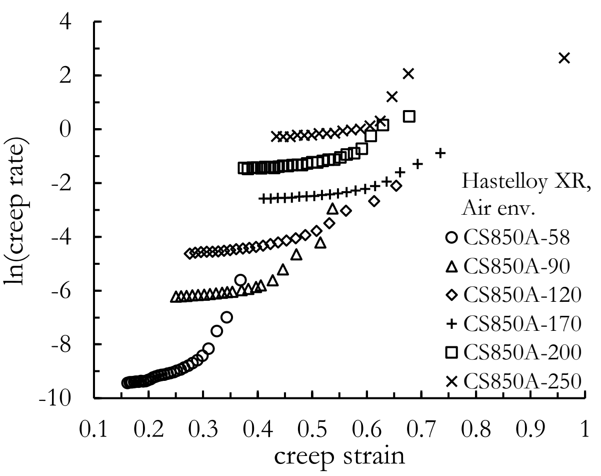

Fig. 6. Tertiary creep rate versus creep strain at 850°C.

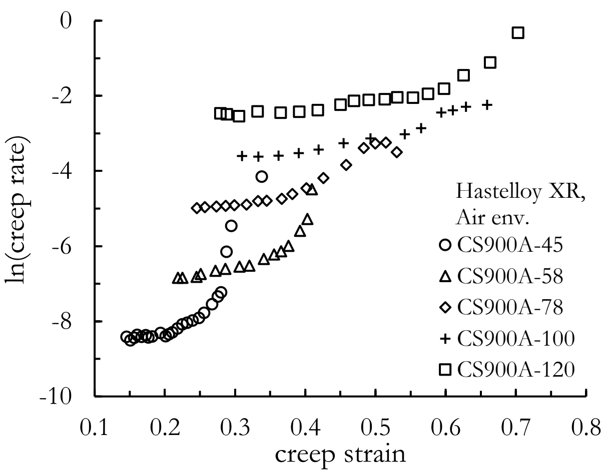

Fig. 7. Tertiary creep rate versus creep strain at 900°C.

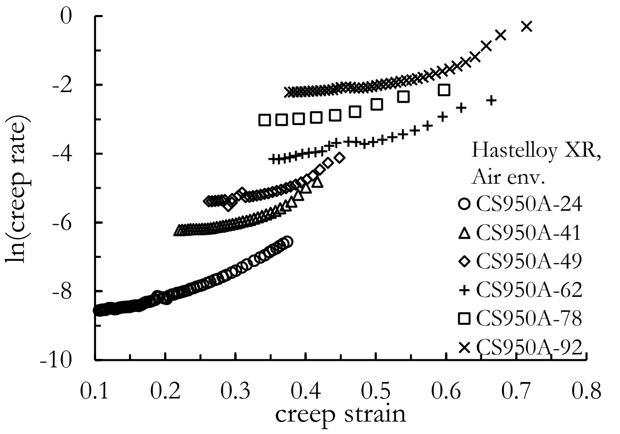

Fig. 8. Tertiary creep rate versus creep strain at 950°C.

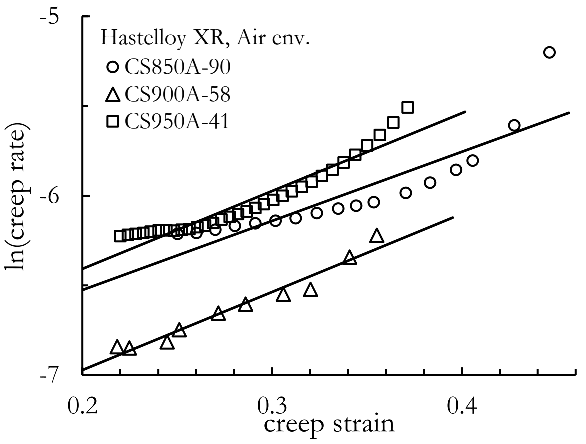

Fig. 9. Examples of Ω and $\dot{\varepsilon}_0$ determined by minimizing the MAE of creep strain prediction.

where N_{ter} is the amount of data in the tertiary stage, and ε_{pred} and ε_{exp} are the predicted and experimental creep strain, respectively. The values of Ω and $\dot{\varepsilon}_0$ from the group with the lowest MAE were chosen. Figure 9 depicts examples of applying this procedure to determine Ω and $\dot{\varepsilon}_0$. Figure 10 shows the prediction of tertiary stage creep strain for the cases shown in Fig. 9. The representative Ω and $\dot{\varepsilon}_0$ values for the test conditions listed in Table 1 are summarized in Table 2. The low Ω values under the investigated conditions indicate the presence of ductile creep. The tertiary stage then begins with high strain and low strain rate acceleration. An Arrhenius equation was usually used to express temperature dependence, whereas power function [17,18] or hyperbolic sine function [5, 6] were used to express stress dependence. After examining these empirical forms, the hyperbolic sine function was shown to be inaccurate for this alloy. Moreover, slight improvement in the correlation was found after normalizing the applied stress with the Young's modulus at temperature. As a result, the following empirical functions were proposed.

$$\Omega(\sigma,T) = A_\Omega \cdot \left(\frac{\sigma}{E(T)}\right)^{n_\Omega} \cdot e^{Q_\Omega/RT} \tag{6}$$

$$\dot{\varepsilon}_0(\sigma,T) = A_{\dot{\varepsilon}_0} \cdot \left(\frac{\sigma}{E(T)}\right)^{n_{\dot{\varepsilon}_0}} \cdot e^{Q_{\dot{\varepsilon}_0}/RT} \tag{7}$$

where σ is applied stress (MPa), T is temperature (K), $E(T)$ is Young's modulus (MPa) at temperature T, R is gas constant (8.314 J/mol·K); and A_Ω, n_Ω, Q_Ω, $A_{\dot{\varepsilon}_0}$, $n_{\dot{\varepsilon}_0}$, and $Q_{\dot{\varepsilon}_0}$ are empirical constants. The Young's modulus at a temperature of 850, 900, and 950 °C are 127,490 MPa [22], 94,000 MPa [24], and 72,000 MPa [24], respectively. The empirical constants values obtained from nonlinear regression analysis are listed in Table 3. Equations (6) and (7) can reasonably predict the values of Ω and $\dot{\varepsilon}_0$, as shown in Figs. 11 and 12.

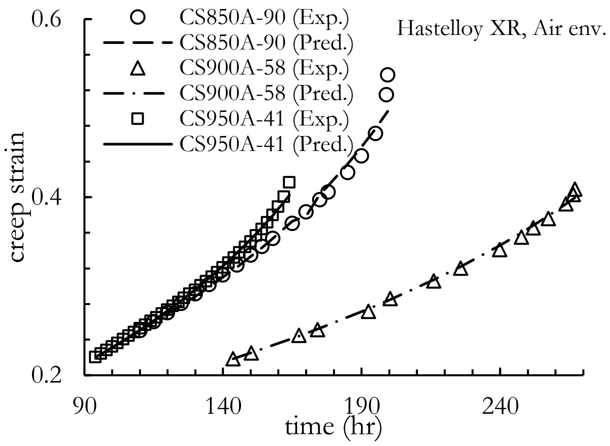

Fig. 10. Prediction of tertiary stage creep strain using Ω and $\dot{\varepsilon}_0$ in Fig. 9.

Table 2. Representative Ω and $\dot{\varepsilon}_0$ values for Hastelloy XR under constant stress uniaxial creep tests in the air environment.

Code	Ω	$\dot{\varepsilon}_0$ (hr^{-1})
CS850A-58	6.679	2.467×10^{-5}
CS850A-90	3.855	6.773×10^{-4}
CS850A-120	3.743	3.147×10^{-3}
CS850A-170	2.457	2.560×10^{-2}
CS850A-200	2.890	7.171×10^{-2}
CS850A-250	2.606	2.283×10^{-1}
CS900A-45	6.414	7.374×10^{-5}
CS900A-58	4.356	3.920×10^{-4}
CS900A-78	4.781	1.809×10^{-3}
CS900A-100	2.828	1.039×10^{-2}
CS900A-120	1.627	4.997×10^{-2}
CS950A-24	6.282	8.552×10^{-5}
CS950A-41	4.342	6.913×10^{-4}
CS950A-49	4.282	1.375×10^{-3}
CS950A-62	4.177	3.467×10^{-3}
CS950A-78	2.684	1.799×10^{-2}
CS950A-92	2.793	3.490×10^{-2}

DOI:10.4186/ej.2023.27.9.15

Table 3. Best-fit coefficients of the empirical equations for the model parameters.

Parameter	Coefficient	Value
Ω (Eq. (6))	A_Ω	3.5909×10^{-3}
	n_Ω	-0.7237
	Q_Ω	1.7809×10^{4}
$\dot{\varepsilon}_0$ (hr^{-1}) (Eq. (7))	$A_{\dot{\varepsilon}_0}$	7.2014×10^{15}
	$n_{\dot{\varepsilon}_0}$	5.1314
	$Q_{\dot{\varepsilon}_0}$	-5.6019×10^{4}

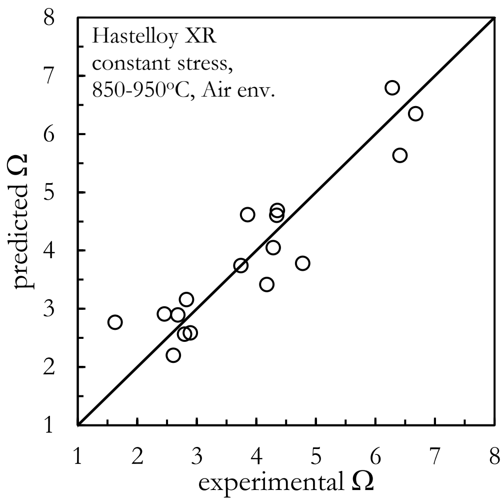

Fig. 11. Comparison of Ω predicted by Eq. (6) with the experimental one.

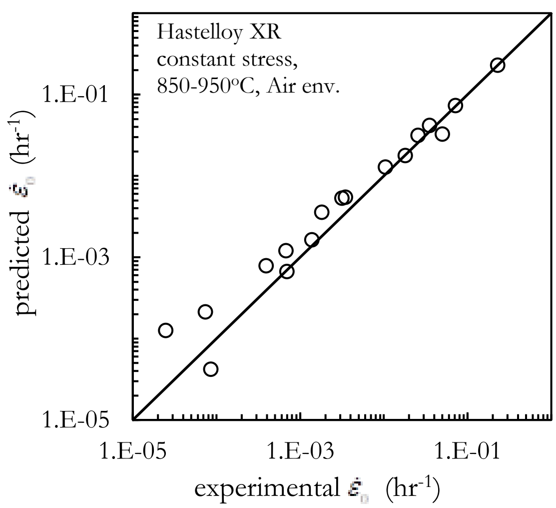

Fig. 12. Comparison of $\dot{\varepsilon}_0$ predicted by Eq. (7) with the experimental one.

4. Creep Life Prediction

This section explains the applicability of the Ω method to a remaining creep life prediction under three scenarios, i.e., constant stress, constant load, and simulated continuous monitoring.

4.1. Constant Stress Cases

The creep data set used in the investigation was the same data set used to develop the empirical equations for the model parameters. The Ω and $\dot{\varepsilon}_0$ values were calculated by Eqs. (6) and (7) under the applied stresses and temperatures listed in Table 1. The remaining life in consideration was defined as a time interval between the onset of the tertiary creep stage to the rupture time, i.e., t_r - t_{ter}. The remaining life was predicted by using Eq. (3) and ε^* was substituted with ε_{ter}. The prediction results are listed in Table 4 and graphically compared with the experiments as shown in Fig. 13. Most of the predictions were on the conservative side and within a factor of 2 range.

Table 4. Comparison of predicted remaining life with experimental results under constant stress creep tests.

Code	Remaining life $t_r - t_{ter}$ (hr)	
	experiment	Prediction
CS850A-58	1396.80	328.41
CS850A-90	89.40	41.69
CS850A-120	21.30	13.56
CS850A-170	2.93	2.02
CS850A-200	0.83	1.09
CS850A-250	0.30	0.52
CS900A-45	499.90	243.79
CS900A-58	123.40	57.88
CS900A-78	25.90	19.29
CS900A-100	8.60	6.21
CS900A-120	3.60	3.53
CS950A-24	765.00	1427.44
CS950A-41	70.00	10.76
CS950A-49	29.00	27.64
CS950A-62	11.00	10.42
CS950A-78	4.00	3.77
CS950A-92	2.05	2.07

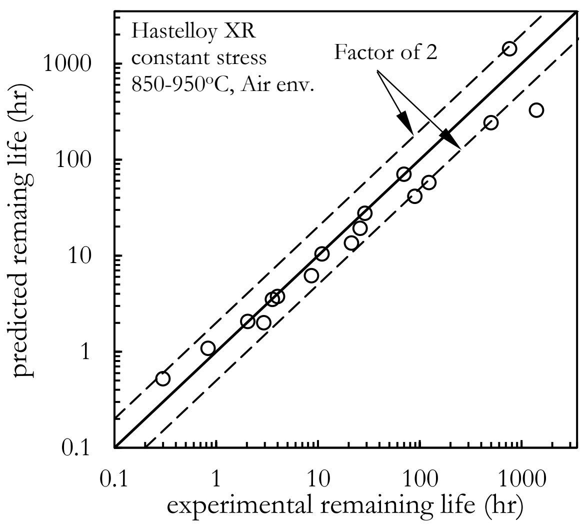

Fig. 13. Comparison of predicted remaining life in experiments under constant stress creep tests.

There are two reasons for using Eq. (3) in a remaining life prediction rather than a usual expression $1/\dot{\varepsilon}_0\Omega$. First, the tertiary creep stage begins around 50% of the rupture life. It is erroneous to assume that the strain at the onset of the tertiary creep stage is close to zero, which causes the first term in the denominator to be close to 1. Second, the Ω values for Hastelloy XR are quite low when compared to other kinds of steel [15-19], which have values in the tens. As a result, it is inappropriate to ignore the second term in the denominator.

4.2. Constant Load Cases

Because components may operate under load-controlled conditions, it is necessary to study a modification of the model developed based on constant stress creep data when applying to a constant load condition. This section proposed a simple modification and verified it with data from the literature [23, 26].

Under constant loading, stress increases as the specimen elongates. The relationship between the actual stress and axial strain can be derived as follows if the extension is uniform (i.e., no necking), and the constant volume assumption is used.

$$\sigma(t) = \sigma_{init} \cdot e^{\varepsilon(t)} \tag{8}$$

where $\sigma(t)$ and $\varepsilon(t)$ is stress and strain at elapsed time t, and σ_{init} is initial stress (i.e., stress at $t = 0$). The remaining life can be calculated by numerically integrating Eq. (1). If the Euler's method is used, a new creep strain ε_{i+1} is predicted using the current creep rate $\dot{\varepsilon}_i$ to extrapolate linearly over a time step Δt from a current creep strain ε_i. by the following equation.

$$\varepsilon_{i+1} = \varepsilon_i + \dot{\varepsilon}_i \cdot \Delta t \tag{9}$$

where i = 0, 1, 2, …. The current creep rate can be calculated from Eq. (1) using the actual applied stress at the current step σ_i. Finally, Eq. (9) can be written as:

$$\varepsilon_{i+1} = \varepsilon_i + \dot{\varepsilon}_0(\sigma_i, T) \cdot e^{\Omega(\sigma_i, T)\cdot\varepsilon_i} \cdot \Delta t \tag{10}$$

Note that the parameters Ω and $\dot{\varepsilon}_0$ now depend on the actual applied stress, which is calculated by Eq. (8) with the current creep strain. The initial conditions, i.e., i = 0 were set by

$$\varepsilon_0 = \varepsilon_{ter} \tag{11}$$

$$\sigma_0 = \sigma_{init} e^{\varepsilon_{ter}} \tag{12}$$

The calculation using Eq. (10) was repeated until the new creep strain was higher than or equal to the creep ductility, i.e., $\varepsilon_{i+1} \geq \varepsilon_r$. The rupture time was predicted to be $i\cdot\Delta t$. The time step Δt was set to 0.04% of the rupture time, which is sufficiently small to satisfy a convergence criterion of 0.1% or better. The predicted remaining life and experimental results are listed in table 6 and graphically compared in Fig. 14. Most of the predictions lie on the non-conservative side but within a factor of two ranges, which is practically acceptable. One reason might come from the assumption of a uniform deformation which underestimates the applied stress and then the creep rate as a consequence when necking occurs. However, the extension of the empirical equations of Ω model parameters derived from a constant stress creep data to predict a creep life under constant load by the present approach was practically acceptable.

Table 6. Constant load uniaxial creep data in air environment for Hastelloy XR.

Code	Temperature T (°C)	Initial stress σ_0 (MPa)	Rupture time t_r (hr)	Tertiary stage: Onset time t_{ter} (hr)	Tertiary stage: Onset strain ε_{ter}	Creep ductility ε_r	Ref.
CL900A-38a	900	38.00	2567.4	299.6	0.0055	0.4093	26
CL900A-38b		38.00	2112.3	74.0	0.0022	0.3477	26
CL900A-47a		47.00	657.8	23.9	0.0011	0.3849	26
CL900A-47b		47.00	325.4	23.7	0.0073	0.5231	26
CL900A-58a		58.00	172.5	24.0	0.0092	0.6444	26
CL900A-58b		58.00	80.3	23.7	0.0652	0.6868	26
CL950A-20	950	19.99	1443.9	612.0	0.0945	0.3310	23
CL950A-22a		22.00	2566.4	142.0	0.0030	0.3263	26
CL950A-22b		22.00	2830.3	141.8	0.0030	0.3219	26
CL950A-24		23.99	833.4	360.0	0.0937	0.3201	23
CL950A-29		29.03	437.8	123.0	0.0581	0.3454	23
CL950A-30a		30.00	431.5	19.9	0.0300	0.4606	26
CL950A-30b		30.00	387.6	24.0	0.1310	0.5805	26
CL950A-34		34.02	161.0	69.0	0.1046	0.3746	23
CL950A-40a		40.02	82.7	27.0	0.0797	0.3975	23
CL950A-40b		40.00	110.4	19.9	0.0024	0.5644	26
CL950A-40c		40.00	116.3	24.0	0.0298	0.6217	26

DOI:10.4186/ej.2023.27.9.15

Table 7. Comparison of predicted remaining life with experimental results under constant load creep tests.

Code	Remaining life $t_r - t_{ter}$ (hr)	
	Experiment	Prediction
CL900A-38a	2267.8	966.4
CL900A-38b	2038.3	985.2
CL900A-47a	633.9	365.0
CL900A-47b	301.7	351.4
CL900A-58a	148.5	128.0
CL900A-58b	56.6	77.6
CL950A-20	831.9	1555.2
CL950A-22a	2424.4	3008.9
CL950A-22b	2688.5	3003.5
CL950A-24	473.4	700.2
CL950A-29	314.8	450.1
CL950A-30a	411.6	732.2
CL950A-30b	363.6	650.2
CL950A-34	92.0	138.7
CL950A-40a	55.7	85.6
CL950A-40b	90.5	183.3
CL950A-40c	92.3	143.4

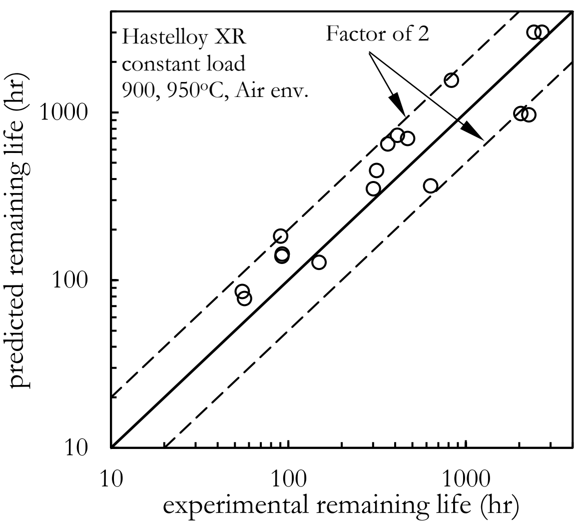

Fig. 14. Comparison of predicted remaining life with experiments under constant load creep tests.

4.3. Simulated Continuous Monitoring of the Remaining Life

This section investigated the applicability of the Ω method in predicting the remaining life when the creep data is collected sequentially. For demonstration, two creep tests, CS850A-58 and CL950A-20 were chosen. It should be noted the values for Ω, and $\dot{\varepsilon}_0$ in this scenario can be calculated directly from the collected data up to the assessment time without using Eqs. (6) and (7).

There were two simulation schemes considered as shown in Fig. 15. Both schemes start with the data point located at the onset of the tertiary creep stage. As data collection progresses, the most recent collected data will be denoted as a current point. Once the strain at the current point has increased sufficiently from the starting point as shown in Fig. 15(a), the model parameters can be determined, and the remaining life is predicted. When a new set of data points becomes available, the procedures are repeated. For the first scheme, the current set of data is analyzed in a combination with the previous sets of data, as shown in Fig. (15b). In the second scheme, however, only the current set of data is analyzed. For both schemes, the remaining life is defined as the time interval between the current point and the rupture time. The remaining life was predicted by Eq. (3) with ε^* equal to strain at the current point. The confidence interval for the remaining life was estimated from a standard error of each parameter by a Monte Carlo simulation.

4.3.1. Case 1: CS850A-58

The tertiary creep data was divided into 5 sets for the first simulation scheme, as shown in Table 8. Columns 2 and 3 of the table list the creep strains at the first and current points of each data set. The strain at the current point of each data set is chosen to increase by approximately 10% from the previous one, in which the authors considered sufficient to cover the strain measurement uncertainty. The Ω model parameters for each data set were determined by fitting Eq. (4) to the data using a least-square regression. The values for parameters Ω and $\ln\dot{\varepsilon}_0$, as well as their standard errors (SE), are listed in columns 4-7. Equation (3) was used to calculate the remaining life from the last point of each data set using the corresponding values of model parameters and strain at the last point, and the results are listed in column 8. The next step was a determination of the uncertainty of the remaining life due to data scatter

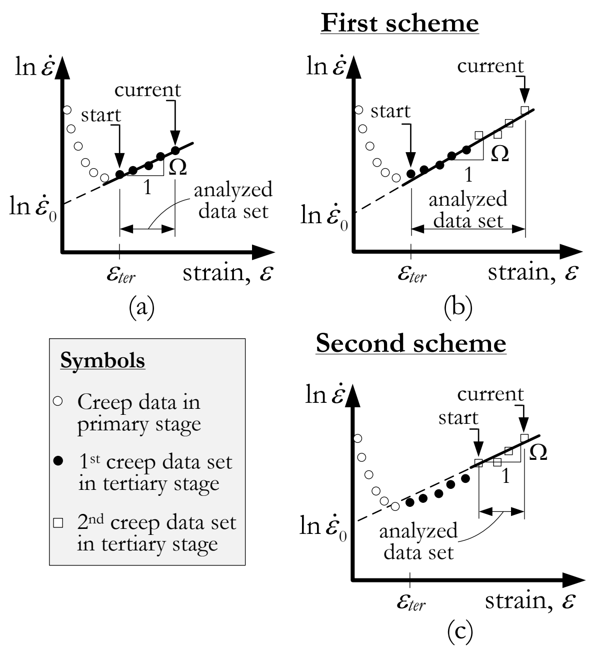

Fig. 15. Schemes for repeated analysis of Ω model parameters.

Table 8. Continuous prediction of remaining life using the first scheme for the CS850A-58 test.

Set	Creep strain		Model parameters		Standard error		Remaining life (hr.)				
							Eq. (3)	Monte Carlo			Exp.
	1st point	Current point	Ω	$\ln\dot{\varepsilon}_0$	SE_Ω	$SE_{\ln\dot{\varepsilon}_0}$		Mean	SD	95% CI	
1	0.1618	0.1781	2.558	-9.843	0.568	0.097	1801.8	1827	330	(1265, 2554)	1196.8
2	0.1618	0.1994	2.296	-9.799	0.225	0.041	1600.3	1605	120	(1382, 1852)	946.8
3	0.1618	0.2242	4.652	-10.217	0.439	0.084	1015.0	1026	155	(755, 1361)	696.8
4	0.1618	0.2526	5.151	-10.309	0.244	0.050	714.3	718	64	(600, 851)	446.8
5	0.1618	0.2898	6.244	-10.523	0.265	0.059	379.2	381	40	(308, 465)	196.8

Using the Monte Carlo simulation. The simulation assumed Ω and $\ln\dot{\varepsilon}_0$ had normal distributions, with means and standard deviations equal to the least-square fit results and standard errors. The remaining life was calculated using Eq. (3) after generating random values for Ω and $\ln\dot{\varepsilon}_0$. The calculation was repeated 5×10^4 times, and the distribution of remaining life was found to be lognormal, as shown by the histogram in Fig. 16 for data set no. 1. Columns 9-11 show the mean, standard deviation (SD), and (two-tails) 95% confidence interval of the remaining life derived from the distribution.

The remaining life calculated using Eq. (3) was found to be close to the mean of the Monte Carlo simulation. Thus, Eq. (3) can be used to calculate the mean of remaining life in a quick but accurate manner. However, the experimental results deviated significantly from the predicted remaining life (by a factor of 1.5 to 2) and fell outside the 95% confidence interval. This finding suggested that the deviation was caused not only by data scatter but also by the limitation of the Ω model. As shown in Fig. 17, the Ω model based on data sets 1 - 5 could not adequately follow the trend of the experimental results and underestimated the creep rate, causing the predicted life to be longer than the experimental life.

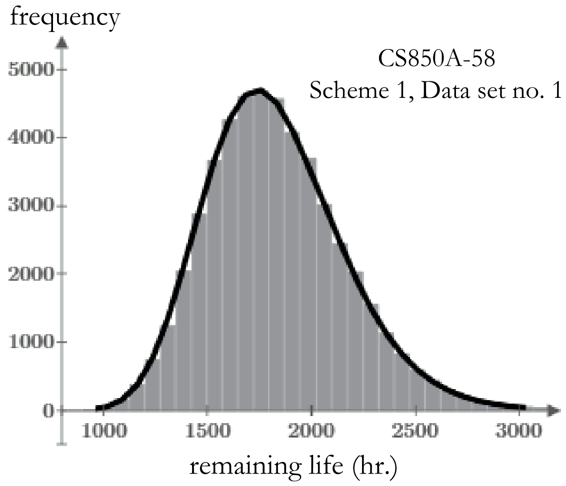

Fig. 16. Lognormal distribution of remaining life from data set no. 1 of CS850A-58.

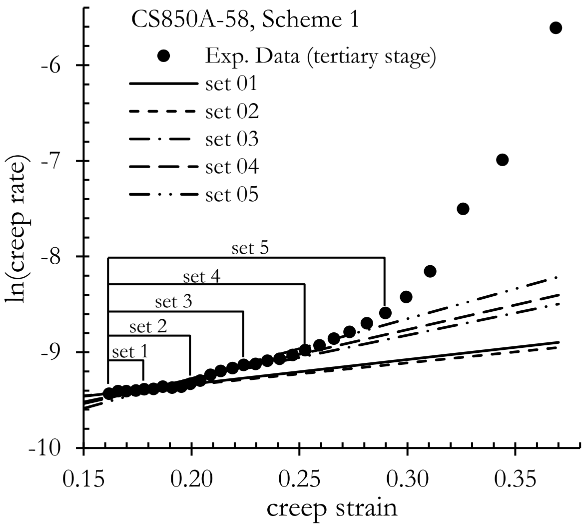

Fig. 17. Ω model parameters for CS850A-58 test determined by the first scheme.

Next, consider applying the second simulation scheme to the same creep data (CS850A-58). Table 9 summarizes the data sets and analysis results. Each set covers an approximate 10% increase in strain. The effect of the data set used on the creep rate prediction model parameters is shown in Fig. 18.

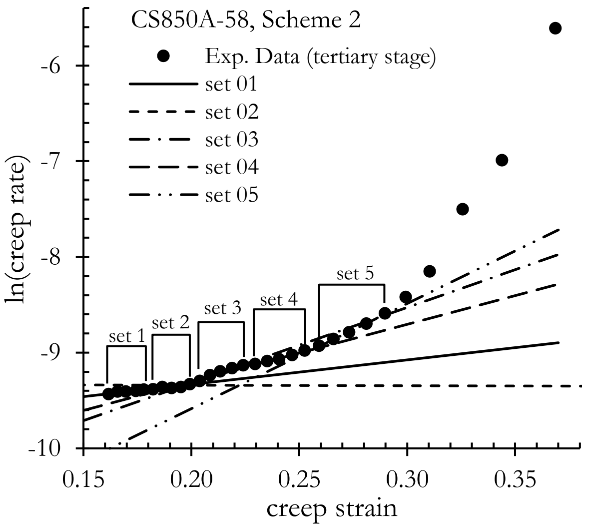

Fig. 18. Ω model parameters for CS850A-58 test determined by the second scheme.

Table 9. Continuous prediction of remaining life using the second scheme for CS850A-58 test.

Set	Creep strain		Model parameters		Standard error		Remaining life (hr.)					
							Eq. (3)	Monte Carlo			Exp.
	1st point	Last point	Ω	$\ln\dot{\varepsilon}_0$	SE_Ω	$SE_{\ln\dot{\varepsilon}_0}$		Mean	SD	95% CI	
1	0.1618	0.1781	2.558	-9.843	0.568	0.097	1801.8	1827	330	(1265, 2554)	1196.8
2	0.1824	0.1994	2.493	-9.838	0.855	0.163	1574.2	1640	480	(897, 2760)	946.8
3	0.2040	0.2242	7.883	-10.893	0.787	0.168	792.4	820	230	(460, 1354)	696.8
4	0.2296	0.2526	5.996	-10.503	0.447	0.108	670.3	679	116	(479, 933)	446.8
5	0.2593	0.2898	10.983	-11.782	0.303	0.083	286.6	289	37	(223, 368)	196.8

According to Table 9, the predicted remaining life using Eq. (3) is also close to the mean of the Monte Carlo simulation. Moreover, this scheme improved the prediction of the remaining life. The reason for this could be that the best-fit line can adjust to the current deformation state better than the first scheme, as shown in Fig. 18. The standard errors of this scheme were higher than the first since the amount of data in each set was smaller, resulting in a wider confidence interval than the first scheme. Because of better predictions and wider confidence interval, the experimental results tended to fall within or close to the confidence interval.

To summarize, it is preferable to determine the model parameters for this case study using a set of data that represents the current deformation state. Moreover, the data set should contain an adequate amount of data and cover a sufficient range of strain.

4.3.2. Case 2: CL950A-20

For a CL950A-20 test, only the second scheme was considered because it performed better than the first. Table 10 summarizes the findings. Similar conclusions can be drawn. First, the life predicted by Eq. (3) agreed with the mean of the Monte Carlo simulation. Next, the scheme accurately predicted the remaining life when compared to the experimental results. Finally, several experimental results fell within the 95% confidence interval. Figure 19 shows the benefit of the second scheme in adapting the Ω model as a new data set is collected.

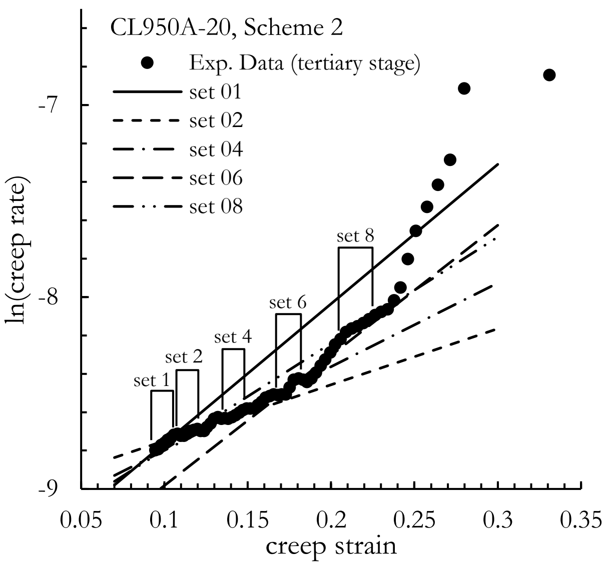

Fig. 19. Ω model parameters for CL950A-20 test determined by the second scheme.

Table 10. Continuous prediction of remaining life using the second scheme for CL950A-20 test.

Set	Creep strain		Model parameters		Standard error		Remaining life (hr.)					
							Eq. (3)	Monte Carlo			Exp.
	1st point	Current point	Ω	$\ln\dot{\varepsilon}_0$	SE_Ω	$SE_{\ln\dot{\varepsilon}_0}$		Mean	SD	95% CI	
1	0.0945	0.1058	7.261	-9.488	0.321	0.032	678.7	680	47	(592, 776)	756
2	0.1078	0.1197	2.918	-9.041	0.750	0.085	938.6	950	170	(660, 1324)	672
3	0.1216	0.1341	6.445	-9.486	0.987	0.126	619.4	635	155	(384, 988)	588
4	0.1363	0.1494	4.358	-9.235	0.497	0.071	670.5	675	91	(514, 870)	504
5	0.1515	0.1655	5.906	-9.482	0.499	0.079	521.6	527	75	(395, 688)	420
6	0.1680	0.1832	6.777	-9.660	1.219	0.214	422.7	450	172	(203, 866)	336
7	0.1856	0.2025	11.783	-10.640	0.360	0.070	254.4	256	29	(203, 317)	252
8	0.2057	0.2265	5.533	-9.348	0.367	0.079	260.1	262	34	(201, 334)	168

5. Conclusions

The remaining creep life prediction for the Hastelloy XR at temperatures of 850, 900, and 950°C in an air environment by the Ω model was studied using a short-term creep data from the literature. The main conclusions obtained from this study are as follows:

1. The values of parameter Ω for the alloy were quite low (in comparison to other kinds of steel). Therefore, predicting remaining life using the simplified expression, i.e., $1/\dot{\varepsilon}_0\Omega$, is not recommended.
2. Based on the constant stress creep data, the dependence of stress and temperature of the model parameters, were found to be expressed appropriately by a power law and Arrhenius equation, respectively. The validity range of the proposed empirical equations for the model parameter should be restricted to the conditions studied. Additional experiments should be carried out to evaluate the applicability of the equations or to introduce modifications when applying beyond the scope of the present study, such as long-term creep behavior (e.g., creep under lower applied stress or temperature), multiaxial creep behavior, and creep under variable stress or temperature.
3. Remaining creep life prediction under constant load could be done by incorporating the effect of increasing stress as the specimen elongated into the creep constitutive equation and calculating the model parameters based on the actual applied stress.
4. In most cases, the Ω model could predict the remaining life under constant stress and constant load within a factor of 2.
5. The Ω model could be employed for continuous monitoring of the remaining life without prior knowledge of the model parameters. The model parameters could be calculated based on the acquired data, but it was recommended to use a current set of data. The remaining life predicted by this scheme was within a factor of 2. Probabilistic analysis using a Monte Carlo simulation provided a confidence interval for the remaining life, which may enhance decision making.

Acknowledgement

This research did not receive any specific grant from funding agencies in the public, commercial, or not-for-profit sectors.

References

[1] R. Viswanathan, *Damage Mechanisms and Life Assessment of High-Temperature Components*. ASM International, 1989, pp. 99-101.

[2] A. K. Ray, Y. N. Tiwari, P. K. Roy, S. Chaudhuri, S. C. Bose, R. N. Ghosh, and J. D. Whittenberger, "Creep rupture analysis and remaining life assessment of 2.25Cr–1Mo steel tubes from a thermal power plant," *Mater. Sci. Eng. A*, vol. 454–455, pp. 679-684, 2007.

[3] F. F. M. dos Santos, H. C. Furtado, and L. H. de Almeida, "Remaining life evaluation based on strain deformation monitoring," *J. Fail. Anal. Prev.*, vol. 18, pp. 809–818, 2018.

[4] R. Bonetti, A. Morris, P. H. Shipway, and W. Sun, "Empirical relationships between hardness, replica and strain and their roles in health monitoring based life assessment for aged power plant materials," *Int. J. Pres. Ves. Pip.*, vol. 199, p. 104735, 2022.

[5] H. Zhang, J. Jia, N. Wang, X. Hu, S. -T. Tu, S. Zhou, and Z. Wang, "Development of on-line monitoring systems for high temperature components in power plants," *Sensors*, vol. 13, no. 11, pp. 15504-15512, 2013.

[6] H. Nishida, "Development of on-line creep monitoring system by using new small-scale high temperature strain gages," *Trans. Jpn. Soc. Mech. Eng. A*, vol. 75, no. 753, pp. 690-692, 2009.

[7] A. Morris, C. Maharaj, M. Kourmpetis, I. Dear, A. Puri, and J. Dear, "Optical strain measurement techniques to assist in life monitoring of power plant components," *ASME J. Press. Vessel Technol.*, vol. 131, no. 2, p. 0224502, 2009.

[8] J. Corcoran, P. Hooper, C. Davies, P. B. Nagy, and P. Cawley, "Creep strain measurement using a potential drop technique," *Int. J. Mech. Sci.*, vol. 110, pp. 190-200, 2016.

[9] S. R. Holdsworth, "Constitutive equations for creep curves and predicting service life," in *Creep-Resistant Steels*. Woodhead Publishing, 2008, ch. 14, pp. 403-420.

[10] A. Kondyr, R. Sandstroem, and A. Samuelsson, "Creep deformation, creep damage accumulation and residual life prediction for three low alloyed CrMo-steels," SIMR, Sweden, Stockholm, Rep. SVF-67, 1979.

[11] B. J. Cane, "Remaining creep life estimation by strain assessment on plant," *Int. J. Pres. Ves. Pip.*, vol. 10, no. 1, pp. 11-30, 1982.

[12] M. Prager, "Development of the MPC omega method for life assessment in the creep range," *ASME. J. Pressure Vessel Technol.*, vol. 117, no. 2, pp. 95-103, 1995.

[13] *Fitness-For-Service*, API 579-1/ASME FFS-1, American Petroleum Institute, American Society of Mechanical Engineers, NY, USA, 2016.

[14] C. C. Manu, "Finite element analysis of stress rupture in pressure vessels exposed to accidental fire loading," M.S. thesis, Mechanical and Materials Eng. Dept., Queen's Univ., Canada., Ontario, 2008.

[15] S. Fujibayashi, M. Miura, and K. Togashi, "Life prediction of low alloy ferritic steels based upon the tertiary creep behavior," *ISIJ Int.*, vol. 44, no. 5, pp. 919-926, 2004.

[16] I. Nonaka, S. Torihata, S. Kihara, H. Umaki, and K. Maruyama, "Evaluation of creep residual life for modified 9Cr-1Mo steel based on omega method," *J. Mater. Sci.*, vol. 46, no. 4, pp. 438-442, 1997.

[17] K. S. Park, D. S. Bae, S. K. Lee, G. H. Lee, J. H. Kim, and T. Endo, "Creep modeling for life evaluation and strengthening mechanism of tungsten alloyed 9–12% Cr steels," *Met. Mater. Int.*, vol. 12, no. 5, pp. 385-391, 2006.

[18] I. D. Park, F. Masuyama, and T. Endo, "Creep behavior analysis of 25Cr-20Ni stainless steels with a special reference to tertiary creep, *J. Japan Inst. Metals*, vol. 64, no. 12, pp. 1181-1188, 2000.

[19] J. T. Yeom, J. Y. Kim, Y. S. Na, and N. K. Park, "Creep strain and creep-life prediction for alloy 718 using the omega method," *Met. Mater. Int.*, vol. 9, no. 6, pp. 555–560, 2003.

[20] Y. Fujiwara, M. Goto, K. Iigaki, T. Iyoku, H. Q. Ho, T. Kawamoto, et al., "Design of high temperature engineering test reactor (HTTR)," in *High temperature Gas-Cooled Reactors*. Elsevier, 2021, ch. 2, pp. 60.

[21] M. Prager, "The omega method—An engineering approach to life assessment," *ASME. J. Pressure Vessel Technol.*, vol. 122, no. 3, pp. 273-280, 2000.

[22] Y. Kaji and Y. Muto, "Creep curve formularization by constant stress creep tests," JAERI, Japan, Rep. JAERI-M 89-210, 1989.

[23] Y. Kaji and Y. Muto, "Creep curve formularization at 950^{o}C by constant stress creep tests," JAERI, Japan, Rep. JAERI-M 91-023, 1991.

[24] K. Kikuchi, H. J. Penkalla, and H. Nishi, "Creep constitutive equation in Hastelloy XR: for cases of 900 and 950^{o}C," *Trans. Jpn. Soc. Mech. Eng. A*, vol. 63, no. 613, pp. 2032-2037, 1997.

[25] ATSM, "ASTM E647-13a Standard test methods for measurement of fatigue crack growth rates," in *ASTM Vol. 03.01: Metals−Mechanical Testing; Elevated and Low-Temperature Tests; Metallography*. PA, USA: ASTM International, 2013.

[26] H. Tsuji, T. Tanabe, T. Nakanishi, Y. Nakasone, and H. Nakajima, "Evaluation of the same heat Hastelloy XR as the material used for high-temperature components of the high-temperature engineering test reactor (second report: Evaluation of short-time strength properties for base metal," JAERI, Japan, Rep. JAERI M-93-209, 1993.

Surat Kwanmuang received his B.Sc. in mechanical engineering from Chulalongkorn University, Bangkok, Thailand in 2004, M.Eng and a Ph.D. in Mechanical Engineering from University of Michigan Ann Arbor. Since 2015, Surat Kwanmuang has been serving as a faculty member in the Department of Mechanical Engineering at Chulalongkorn University. He was promoted to the position of assistant professor in 2023. His research interests are Mobile Robots, Localization and Tracking and Estimations in various applications.

Jirapong Kasivitamnuay received his B. Eng. and M. Eng. degrees from Chulalongkorn University, and doctoral degree in mechanical engineering from The University of Tokyo. Since 2000, he has been a faculty member at the Department of Mechanical Engineering, Chulalongkorn University. At present, he is an associate professor. His research interest is fracture mechanics, fatigue, creep, and development of a classroom demonstration rigs for the mechanics of materials course.